Int J Adv Manuf Technol (2003) 22: 626–632
DOI 10.1007/s00170-003-1550-0

ORIGINAL ARTICLE

Yong Huang · Steven Y. Liang

Force modelling in shallow cuts with large negative rake angle and large nose radius tools—application to hard turning

Received: 1 July 2002 / Accepted: 4 October 2002 / Published online: 2 August 2003

Abstract In finish turning, the applied feedrate and depth of cut are generally very small. In some particular cases, such as the finishing of hardened steels, the feedrate and depth of cut are much smaller than tool nose radius. If a tool with a large tool nose radius and large negative rake angle is used in finish turning, the ploughing effect is pronounced and needs to be carefully addressed. Unfortunately, the ploughing effect has not yet been systematically considered in force modelling in shallow cuts with large negative rake angle and large nose radius tools in 3-D oblique cutting. In this study, in order to model the forces in such shallow cuts, first the chip formation forces are predicted by transforming the 3-D cutting geometry into an equivalent 2-D cutting geometry, then the ploughing effect mechanistic model is proposed to calculate the total 2-D cutting forces. Finally, the 3-D cutting forces are estimated by a geometric transformation. The proposed approach is verified in the turning of hardened 52100 steel, in which cutting conditions are typified as shallow cuts with negative rake angle and large nose radius tools. The workpiece material property of hardened 52100 steel is represented by the Johnson-Cook equation, which is determined from machining tests. The comparison between the experimental results and the model predictions is presented.

Nomenclature

$A_{cutting}$	Cutting cross section area
a_0, a_1, a_2, a_3	Constants of the ploughing effect coefficient K_c
b_0, b_1, b_2, b_3	Constants of the ploughing effect coefficient K_t
C_s	Side cutting edge angle
C_s^*	Equivalent side cutting edge angle
d	Depth of cut
F_c^*, F_t^*	Tangential and thrust chip formation forces
F_c, F_t	Total cutting forces with the ploughing effect considered
f	Feedrate
i^*	Equivalent inclination angle
K_c, K_t	Ploughing effect coefficients
P_1, P_2, P_3	Forces in cutting, axial and radial directions
$P_{1,m}$, $P_{2,m}$, $P_{3,m}$	Measured 3-D cutting forces
$P_{c,measure}$, $P_{t,measure}$	Measured 2-D cutting forces
$P_{1,p}$, $P_{2,p}$, $P_{3,p}$	Predicted 3-D cutting forces
$P_{c,prediction}$, $P_{t,prediction}$	Predicted 2-D cutting forces
r	Tool nose radius
t^*	Equivalent undeformed chip thickness
$t_{\max}$	Maximum undeformed chip thickness along the tool nose
T	Temperature
T_m	Melting point temperature
T_r	Reference temperature for measuring σ_0
w^*	Equivalent width of cut
α_n	Cutting edge normal rake angle
α_n^*	Equivalent cutting edge normal rake angle
ε	Uniaxial (effective) strain
$\dot{\varepsilon}$	Strain rate
η_c^*	Equivalent chip flow angle
σ	Flow stress

Y. Huang · S. Y. Liang (✉)
George W. Woodruff School of Mechanical Engineering,
Georgia Institute of Technology, Atlanta,
GA 30332-0405, USA
E-mail: steven.liang@me.gatech.edu

1 Introduction

Force modelling in metal cutting is important for thermal modelling, tool life estimation, chatter prediction,

and tool condition monitoring purposes. Numerous efforts have been devoted to capture the force profiles in metal cutting. Besides laborious experimental approaches, numerous numerical and analytical approaches have been proposed to model the chip formation forces. Although some successes have been achieved in modelling the chip formation forces in metal cutting by the finite element method (FEM), it is not readily applicable because it is laborious and not easy to extend to practical 3-D turning cases [1,2]. Alternatively, analytical models have been favoured as force models in metal cutting because they are easier to implement and can give much more insight about the physical behaviour in metal cutting. To model analytically the chip formation forces in metal cutting, two fundamental approaches have been extensively researched: the minimum energy principle [3,4] and slip line field theory [5]. Numerous researchers have applied or modified these two approaches to model the forces in metal cutting on these bases.

In finish turning, feedrate and depth of cut are generally very small. In some particular cases, such as finishing hardened steels, the feedrate and depth of cut are much smaller than the tool nose radius and the ploughing effect (rubbing effect) is rather pronounced. Furthermore, when undeformed chip thickness is small enough, the ploughing effect contributes to a greater portion of the total cutting forces. Generally this critical chip thickness is defined by the tool nose radius, machine tool system stiffness, and negative rake angle. The ploughing effect needs to be carefully addressed under these cutting configurations. The first study on the ploughing effect in metal cutting was documented by Albrecht [6] in an attempt to estimate the real value of friction coefficient on the tool-chip interface and to explain the paradox of the variation of the friction coefficient with the variation of rake angle. After Albrecht's study, significant efforts have been devoted to model the ploughing force in orthogonal cutting [7,8,9,10]. Unfortunately, no documented effort has been found to deal with this ploughing effect in modelling forces in such shallow cuts with a large negative rake angle and large nose radius under a 3-D oblique cutting condition.

Finish hard turning is a typical turning process using shallow cuts with negative rake angle CBN or ceramic tools. The cutter usually has a large nose radius compared with practical feedrate and depth of cut and has a large negative rake angle. In these situations the ploughing effect can prevail. Material side flow can also be observed as the result of the ploughing effect in hard turning [11]. In this paper, to model cutting forces in such shallow cuts, first the chip formation forces are predicted by transforming the 3-D cutting geometry into an equivalent 2-D cutting geometry [5,12,13]. Then, a ploughing effect mechanistic model is proposed to calculate the total 2-D cutting forces. Finally, 3-D cutting forces are estimated by a geometric transformation. The proposed approach is verified in a machining test of finishing hardened 52100 steel. Here, the workpiece material property is represented by the Johnson-Cook equation, which is determined by independent machining tests.

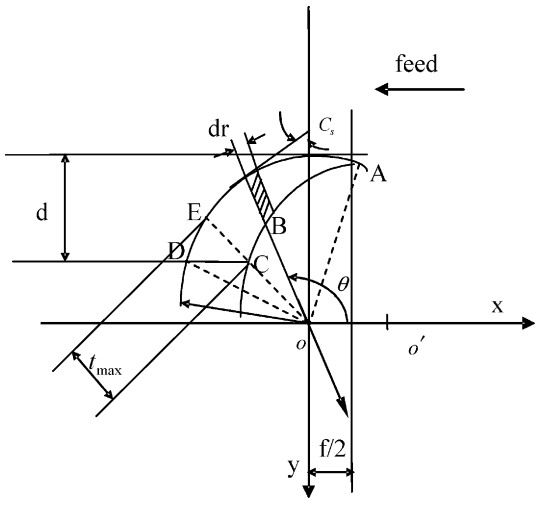

Fig. 1 Cutting geometric model under shallow cuts with a large nose radius tool (o' is the tool nose centre of the previous revolution)

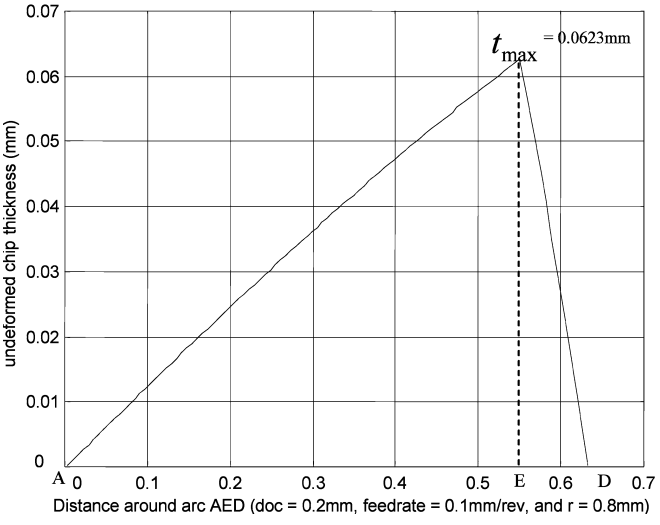

Fig. 2 The undeformed chip thickness around the tool cutting edge AED for one cutting condition

2 Modelling the ploughing effect on cutting forces

Under the shallow cut condition, for a tool with large tool nose radius, the shape of the undeformed chip cross section is not ideally rectangular. By assuming zero rake and inclination angles for the tool, the typical cutting geometry in turning with shallow cuts is shown in Fig. 1. Figure 2 displays the undeformed chip thickness versus the distance of an arbitrary location from point A to point D for a typical finish hard turning condition. The undeformed chip thickness varies around the cutting

edge (arc AED) from zero (location A) to t_{max} (location E) then to zero (location D) again. The maximum chip thickness t_{max} can be calculated by Eq. 1 based on cutting geometry and tool geometry as shown in Fig. 1.

$$t_{\max} = r - \sqrt{r^2 + f^2 - 2f\sqrt{2rd - d^2}} \tag{1}$$

The ploughing effect contributes to a significant portion of the cutting forces where the undeformed chip thickness is small enough in comparison with a value, which is determined by the tool nose radius, machine tool system stiffness, and tool rake angle. Until now, there has been no available model to predict this value in metal cutting. As seen from Fig. 1, some portions along the cutting edge are small enough for the ploughing effect to be pronounced. Without needing to know that value exactly, a mechanistic model is proposed herein to model the overall effect of the ploughing phenomenon on the total cutting forces. Suppose the tangential chip formation force F_c^* and thrust chip formation force F_t^* are the predicted chip formation forces, without considering the ploughing effect then the total cutting forces in a shallow cut are mechanistically modelled to include the ploughing effect as follows:

$$F_c = K_c F_c^*, \; F_t = K_t F_t^* \tag{2}$$

The coefficients K_c and K_t in Eq. 2 are termed ploughing effect coefficients. Experimental evidence has shown that the dependence of the specific cutting energy on the chip thickness can be well described by a power law relationship [14,15]. Here a power law relation is assumed between the ploughing effect coefficients and $t_{\max}$ on the basis that $t_{\max}$ is dependent on the undeformed chip thickness. Furthermore, a linear relationship between the ploughing effect coefficients and $t_{\max}$ is included. Thus, K_c and K_t are defined as

$$K_c = a_0 - a_1 t_{\max} - a_2 t_{\max}^{a_3}, \; K_t = b_0 - b_1 t_{\max} - b_2 t_{\max}^{b_3} \tag{3}$$

The effect of rake angle is neglected for simplicity, since the rake angle in this study is fixed. A different rake angle value will change a's and b's. K_c and K_t are not sensitive to tool material properties, but are dependent on workpiece material properties.

3 Modelling forces in 3-D oblique cutting condition

3.1 Equivalent 2-D oblique cutting geometry for 3-D oblique cutting condition

In typical finish turning, the orthogonal cutting condition no longer holds in the presence of a substantial tool nose radius and a 3D oblique cutting configuration. By considering the equivalent 2-D oblique cutting geometry in finish turning, the force model for orthogonal cutting [16] is extended to model the chip formation forces. The equivalent cutting geometry, including the equivalent cutting edge normal rake angle α_n^*, the equivalent inclination angle i^*, and the equivalent side cutting edge angle C_s^*, can be calculated from the 3-D oblique cutting geometry transformation model as documented in [5,12,13]. For cutting tools with a substantial tool nose radius, C_s is calculated as the angle between the centre line and tool nose tangential line, which is tangential to the intersection point between half depth of cut and the tool. The use of these equivalent cutting geometries for the development of a 3-D force model is discussed below.

3.2 Three-dimensional oblique force model

Based on Stabler's flow rule [17], the equivalent chip flow angle is:

$$\eta_c^* = i^* \tag{4}$$

In determining the turning forces, an orthogonal cutting model can be applied by assuming that the inclination angle is zero irrespective of its actual value and the rake angle is taken as α_n^* [12]. The equivalent undeformed chip thickness t^* and the equivalent width of cut w^* can be calculated by:

$$t^* = f\cos C_s^*, \;\; w^* = d/\cos C_s^* \tag{5}$$

Based on transformed equivalent cutting conditions t^* and w^*, and the transformed equivalent tool normal rake angle α_n^*, the tangential chip formation force F_c^* and the thrust chip formation force F_t^* are calculated based on the orthogonal cutting force model as documented in [16]. With consideration of the ploughing effect on the total cutting forces, the total cutting forces F_c and F_t within the 2-D equivalent cutting geometry can be calculated based on Eq. 2. As shown in Eq. 1, $t_{\max}$ is determined by given process attributes, r, f, and d.

Referring to [12,13] with a single-point cutting tool, the forces acting in the cutting, axial, and radial directions can be calculated respectively from

$$P_1 = F_c, \; P_2 = F_t\cos C_s^* + F_r \sin C_s^*, \; P_3 = F_t \sin C_s^* - F_r \cos C_s^* \tag{6}$$

$$\text{where} \quad F_r = \frac{F_c\left(\sin i^* - \cos i^* \sin\alpha_n^* \tan\eta_c^*\right) - F_t \cos\alpha_n^* \tan\eta_c^*}{\sin i^* \sin\alpha_n^* \tan\eta_c^* + \cos i^*} \tag{7}$$

4 Experimental validation

All machining experiments discussed below are carried out on a horizontal Hardinge lathe with a 7.5 KW spindle, and the workpiece is hardened 52100 bearing steel with a hardness of HRc 62. The forces are measured with a Kistler 9257B dynamometer.

4.1 Determination of the workpiece material properties

The workpiece material property as a function of temperature, strain, and strain rate in the primary and secondary shear zones is needed to model the chip formation forces. Regarding the material property of hardened 52100 bearing steel, several models were researched [18,19], but these models lead to certain contradictions. Poulachon et al. [18] neglected the effect of strain rate for the constitutive relation, but Guo et al. [19] considered strain rate as a dominant factor. The Johnson-Cook equation is used in this study to represent the workpiece material constitutive property and its constants (σ_0, B, n, c, m) are determined based on machining tests. The experimental data is collected by simulating orthogonal cutting of hardened 52100 steel. A Kennametal KD120 CBN grooving insert with 0° rake angle and straight cutting edge is used. To satisfy the plain strain condition, the depth of cut is chosen as 0.889 mm (0.035 in). The experiment is designed based on changing the feedrate from 0.0762 mm/rev to 0.1778 mm/rev at an interval of 0.0254 mm for both cutting velocities of 2.032 m/s (400 sfm) and 3.048 m/s (600 sfm). Since the orthogonal chip formation force model [16] is not analytically differentiable to provide a set of normal equations, the conventional curve fitting method based on least squares method cannot be used here. To overcome this difficulty, the determination of the constants is treated as an optimisation problem by using a genetic algorithm [20]. Based on the experimental cutting force results, the constants of the Johnson-Cook equation are determined by minimizing the difference between measured cutting forces and predicted cutting forces as $\min\left\{\sqrt{\sum\left[\left(F_{c,measure}-F_{c,prediction}\right)^2+w_1\left(F_{t,measure}-F_{t,prediction}\right)^2\right]}\right\}$. Both $P_{c,prediction}$ and $P_{t,prediction}$ are determined by using the orthogonal force model [16]. Since the thrust force is relatively small compared with the tangential cutting force, to compensate the error that may be generated in optimisation, a weight w_1 is added to the thrust force component. In this case, w_1 is specified as 1.2. In this study, the cutting forces when feed rate is 0.1270 mm/rev and 0.1778 mm/rev for both test velocities are used in determining the unknown constants in the Johnson-Cook equation. The resulting Johnson-Cook equation for hardened 52100 bearing steel is

$$\sigma = \left(774.78 + 134.46\varepsilon^{0.3710}\right)\left(1 + 0.0173\ln\dot{\varepsilon}\right) \times \left(1 - \left(\frac{T - T_r}{T_m - T_r}\right)^{3.1710}\right)(Mpa) \quad (8)$$

where $T_m = 1487$°C (1760 K) and $T_r = 25$°C.

Based on the determined Johnson-Cook equation, the cutting forces are predicted by using the orthogonal cutting chip formation force model [16] and are compared with the measured cutting forces in this experiment, which are not used in calibrating the coefficients of Eq. 8. The comparisons are shown in Figs. 3 and 4. In Figs 3 and 4, the data points for feed rates of 0.1270 mm/rev and 0.1778 mm/rev are the results of calibration and the others are for validation. The deviation at a feedrate of 0.0762 mm/rev is believed to result from the cutting edge honing of the grooving insert. Since the grooving inserts used have a straight cutting edge, the undeformed chip thickness is uniform along the cutting edge and is believed to be large enough (except for feedrate of 0.0762 mm) that the ploughing effect will not occur here. No ploughing effect is considered for this grooving process. The comparisons are within 15% when the feedrate is large.

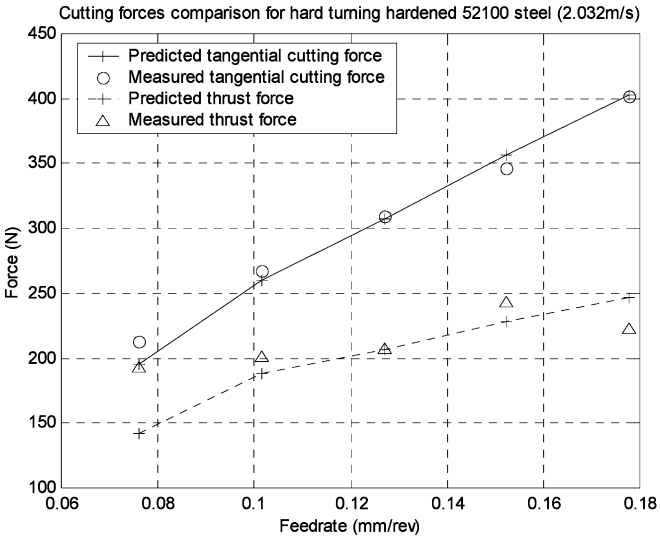

Fig. 3 Cutting forces comparison when turning hardened 52100 steel (velocity = 2.032 m/s and depth of cut = 0.889 mm)

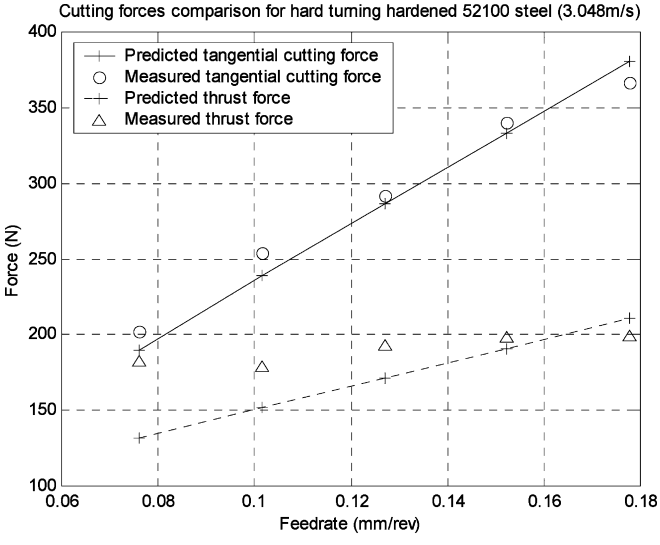

Fig. 4 Cutting forces comparison when turning hardened 52100 steel (velocity = 3.048 m/s and depth of cut = 0.889 mm)

4.2 Calibration of the ploughing effect

A Kennametal CBN tool insert (KD050) is used for turning hardened 52100 steel. The tool has a nose radius of 0.8 mm, chamfer length of 0.1 mm, and chamfer angle of −20°. The normal rake angle on the chamfered face is −25°, the normal rake angle is −5°, and the inclination angle is −5°. The test conditions are selected based on the tool manufacturer's recommended range. Two sets of cutting experiment are performed: (1) Changing the feedrate from 0.0508 mm/rev to 0.1778 mm/rev at an interval of 0.0127 mm/rev by specifying the depth of cut at 0.127 mm and cutting velocity at 2.13 m/s and (2) Changing the depth of cut from 0.1016 mm to 0.3048 mm at an interval of 0.0254 mm by specifying the feedrate at 0.0762 mm/rev and cutting velocity at 2.13 m/s. Because of the difficulty of generating the normal equations for the least squares method, the determination of the constants of the ploughing effect coefficients is treated as an optimisation process. Six groups of experimental results (the 3-D cutting forces when the depth of cut is specified at 0.127 mm and velocity at 21.3 m/s, and feedrate is 0.0508 mm/rev, 0.0762 mm/rev, 0.1016 mm/rev, 0.1270 mm/rev, 0.1524 mm/rev, and 0.1778 mm/rev) are used to determine the constants of the ploughing effect coefficients (a's and b's in Eq. 3) and are solved by minimizing the difference between the measured forces and the predicted forces as $\min\left\{\sqrt{\sum\left[\left(P_{1,m}-P_{1,p}\right)^2+\left(P_{2,m}-P_{2,p}\right)^2+\left(P_{3,m}-P_{3,p}\right)^2\right]}\right\}$. The cutting forces $P_{1,p}$, $P_{2,p}$, and $P_{3,p}$ are predicted based on Eq. 6. Again, a genetic algorithm is used in this calibration. The ploughing effect coefficients of K_c and K_t are determined as

$$K_c = 3.0759 - 1.7424t_{\max} - 6.1909t_{\max}^{0.6592} \quad \text{and}$$
$$K_t = 5.7836 - 2.5969t_{\max} - 14.5324t_{\max}^{0.6246} \qquad (9)$$

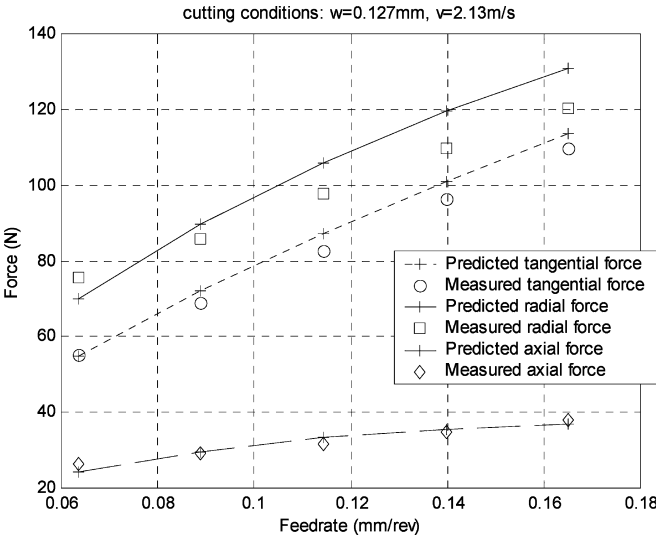

Fig. 5 Cutting forces comparison as feedrate changes (velocity = 2.13 m/s and depth of cut = 0.127 mm)

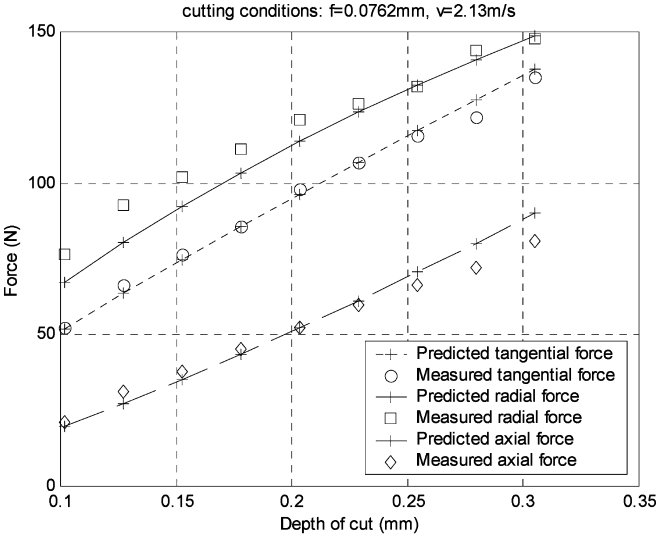

Fig. 6 Cutting forces comparison as depth of cut changes (velocity = 2.13 m/s and feedrate = 0.0762 mm/rev)

4.3 Model validation

As discussed in Section 4.2, six groups of experimental results of the experimental design set one are used in calibrating the ploughing effect coefficients. The remaining data points of experimental design set one (the 3-D cutting forces when the depth of cut is specified at 0.127 mm and velocity at 21.3 m/s, and feedrate is 0.0635 mm/rev, 0.0889 mm/rev, 0.1143 mm/rev, 0.1397 mm/rev, and 0.1651 mm/rev) are used for model validation. These measured cutting forces are compared with the model predictions. As shown in Fig. 5, the comparisons are within 15%.

No experimental data points of experimental design set two are used in the calibration in Section 4.2. To test the feasibility of the proposed mechanistic modelling, the determined ploughing effect mechanistic model (Eq. 9) is further used to predict the total cutting forces for the conditions specified by experimental design set two, where the depth of cut is changed. The predicted forces match well with the experimental data as shown in Fig. 6. The force comparisons are within 15%.

To appreciate the importance of the ploughing effect coefficients, force predictions without considering the ploughing effect are shown in Figs. 7 and 8 for both of the two validation cases. It can be seen that there is a large difference between force predictions and measurements if the ploughing effect is ignored. The values of the ploughing effect coefficients K_c and K_t with respect to feedrate (when depth of cut = 0.127 mm) and depth of cut (when feedrate = 0.0762 mm/rev) are shown respectively in Figs. 9 and 10. As expected, K_c and K_t

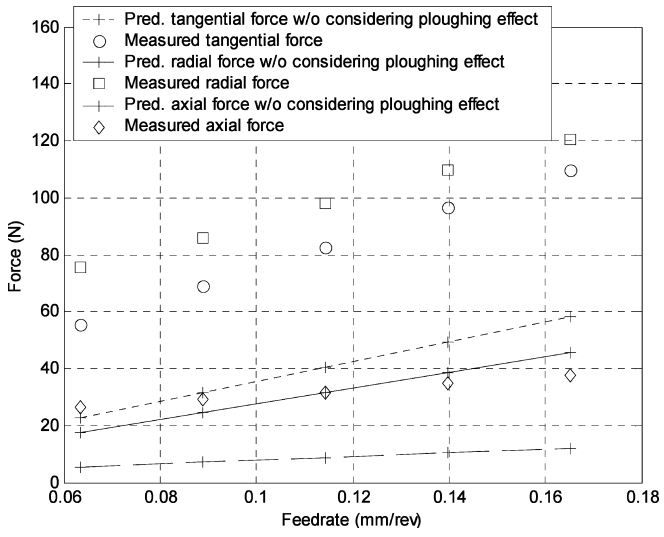

Fig. 7 Cutting forces comparison as feedrate changes without considering the ploughing effect (velocity = 2.13 m/s and depth of cut = 0.127 mm)

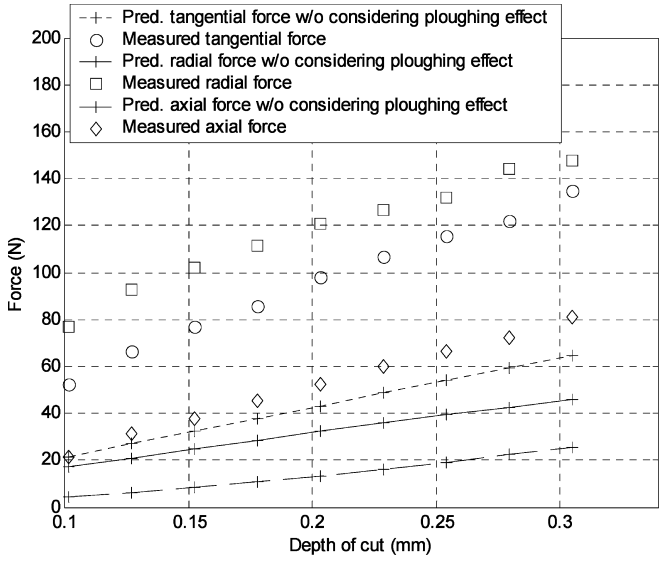

Fig. 8 Cutting forces comparison as depth of cut changes without considering the ploughing effect (velocity = 2.13 m/s and feedrate = 0.0762 mm/rev)

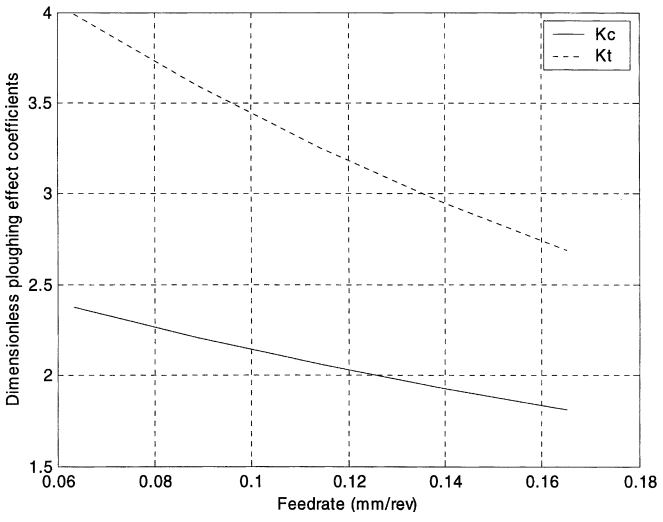

Fig. 9 Ploughing effect coefficients vs. feedrate (depth of cut = 0.127 mm and tool nose radius = 0.8 mm)

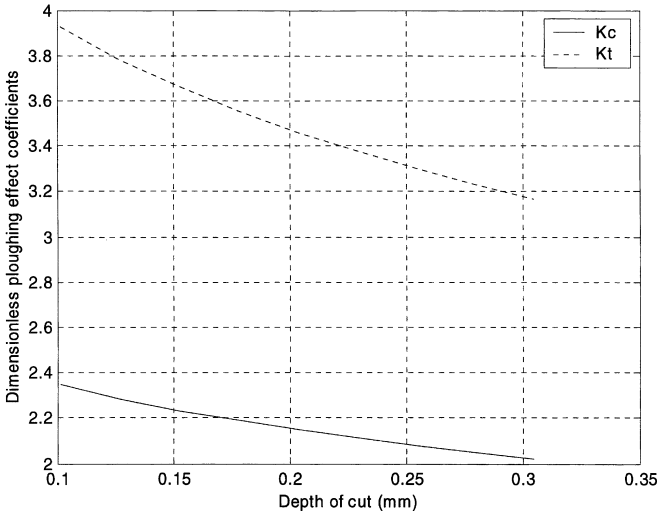

Fig. 10 Ploughing effect coefficients vs. depth of cut (feedrate = 0.0762 mm/rev and tool nose radius = 0.8 mm)

decrease as the feedrate or depth of cut increases because the ploughing effect is less significant when maximum undeformed chip thickness increases. For shallow cuts, the ploughing forces contribute to the dominant portion of the total cutting forces and cannot be ignored as seen from Figs. 9 and 10.

5 Conclusion

The ploughing effect is common in shallow cuts with large negative rake angle and large nose radius tools, such as used in finish hard turning. To model cutting forces in such shallow cuts in this paper, first the chip formation forces are predicted by transforming the 3-D cutting geometry into the equivalent 2-D cutting geometry, then a ploughing effect mechanistic model is proposed to calculate the total 2-D cutting forces. Finally, 3-D cutting forces are estimated by geometric transformation. The proposed model is calibrated and validated using experimental machining data for finish turning hardened 52100 steel. The Johnson-Cook equation is used to represent the workpiece material properties of hardened 52100 steel. The total cutting forces match measurements within 15%. The comparison also indicates the validity of the ploughing effect mechanistic model such as applied to a larger range cutting conditions.

Acknowledgements The authors wish to express their gratitude to Mr. Anand Ramesh at Georgia Tech for the orthogonal hard grooving data and Mr. Ty G. Dawson at Georgia Tech for his discussion during the machining experiments. The authors also thank the reviewers for their inputs and comments.

References

1. Wang BP, Sadat AB, Twu MJ (1988) Finite element simulation of orthogonal cutting: A Survey. Materials in manufacturing processes, MD-vol. 8, ASME WAM, Chicago, pp 87–91
2. Ng EG, Aspinwall DK, Brazil D et al (1999) Modeling of temperature and forces when orthogonally machining hardened steel. Int J Mach Tools Manuf 39:885–903
3. Merchant ME (1945) Mechanics of the metal cutting process, Part 2: Plasticity conditions in orthogonal cutting. J Appl Phys 16:318–324
4. Lee EH, Shaffer BW (1951) Theory of plasticity applied to problems of machining. ASME J App Mech 18(4):104–113
5. Oxley PLB (1989) Mechanics of machining, an analytical approach to assessing machinability. Ellis Horwood, West Sussex, England
6. Albrecht P (1960) New developments in the theory of the metal-cutting process, Part 1: The ploughing process in metal cutting. J Eng Ind 348–358
7. Wu DW (1988) Application of a comprehensive dynamic cutting force model to orthogonal wave-generating process. Int J Mech Sci 30(8):581–600
8. Rubenstein C (1990) The edge force components in oblique cutting. Int J Mach Tools Manuf 30(1):141–149
9. Elanayar S, Shin YC (1996) Modeling of tool forces for worn tools: Flank wear effects. ASME J Manuf Sci Eng 118(3):359–366
10. Waldorf DJ, DeVor RE, Kapoor SG (1998) A slip-line field for ploughing during orthogonal cutting. ASME J Manuf Sci Eng 120(4):693–699
11. Kishawy HA, Elbestawi MA (1999) Effects of process parameters on material side flow during hard turning. Int J Mach Tools Manuf 39:1017–1030
12. Arsecularatne JA, Mathew P, Oxley PLB (1995) Prediction of chip flow direction and cutting forces in oblique machining with nose radius tools. Proc Inst Mech Eng 209(B):305–315
13. Arsecularatne JA, Mathew P,Oxley PLB (2000) Modeling approach, its applications and future directions. Mach Sci Technol 4(3):363–397
14. Sabberwal AJP (1961) Chip section and cutting forces during the milling operation, Annals CIRP 10:197–203
15. Oxley PLB (1963) Rate of strain effect in metal cutting. ASME J Eng Ind 85:339–345
16. Huang Y, Liang SY (2003) Force modeling considering the effect of tool thermal property-application to CBN hard turning. Int J Mach Tools Manuf 43:307–315
17. Stabler GV (1951) The fundamental geometry of cutting tools. Proc Inst Mech Eng 165:14–21
18. Poulachon G, Moisan A, Jawahir IS (2001) On modeling the influence of thermo-mechanical behavior in chip formation during hard turning of 100Cr6 bearing steel. Annals CIRP 50(1):31–36
19. Guo YB,Liu CR (2002) Mechanical properties of hardened AISI 52100 steel in hard machining processes. ASME J Manuf Sci Eng 124(1):1–9
20. Goldberg DE (1989) Genetic algorithm in search, optimization, and machine learning, Addison Wesley, Reading, MA